Indonesian Physical Review
Volume 5 Issue 3, September 2022
P-ISSN: 2615-1278, E-ISSN: 2614-7904

Fabrication of Fe_3O_4/ZnO Nanocomposite by Ultrasonication Wave Method and Its Application for Antibacterial

Anggraini Dwi Oktavia[1*], Lydia Rohmawati[1*]
[1] *Physics department, Faculty Mathematics and Natural Science Universitas Negeri Surabaya, Indonesia*

Corresponding Authors E-mail: lydiarohmawati@unesa.ac.id

Article Info

Article info:
Received: 02-07-2022
Revised: 04-08-2022
Accepted: 12-08-2022

Keywords:
Bacteria; antibacterial; Fe3O4/ZnO nanocomposite; ultrasonication wave method

How To Cite:
A.D. Okatvia and L. Rohmawati, "Fabrication of Fe_3O_4/ZnO Nanocomposite by Ultrasonication Wave Method and Its Application for Antibacterial", Indonesian Physical Review, vol. 5, no. 3, p 177-187, 2022.

DOI:
https://doi.org/10.29303/ipr.v5i3.175

Abstract

The spread of diseases caused by bacteria seriously threatens human health. Alternative materials with antibacterial effects are needed to overcome this problem, such as Fe_3O_4/ZnO. This study aims to determine the activity of the antibacterial inhibition zone on Fe_3O_4/ZnO nanocomposites. The Fe_3O_4/ZnO nanocomposite fabrication used the ultrasonication wave method. Characterization was performed using X-ray diffraction (XRD), Fourier Transforms Infrared (FTIR), and antibacterial activity tests. The results of the XRD analysis showed that the average crystal size was about 42 nm for Fe_3O_4, 36 nm for ZnO, and 39 nm for Fe_3O_4/ZnO. The FTIR results on the nanocomposite showed the characteristics of the Fe-O group at the absorption peak of 874.93 and 691.29 cm^{-1}, while at 436.56 cm^{-1} indicated the presence of Zn-O compound bonds. The Fe_3O_4/ZnO nanocomposite with a weight ratio (1:10) showed good effectiveness in inhibiting S. aureus and E. coli bacteria at concentrations of 0.8 mg/m and 1 mg/ml. Meanwhile, in E. coli bacteria, the average diameter of the inhibition zone was relatively low. Thus Fe_3O_4/ZnO nanocomposite has the potential to be applied in antibacterial applications.

Introduction

Human health is currently facing a significant threat to the spread of diseases caused by pathogenic bacteria. In addition, developing new bacteria resistant to antibiotic drugs also poses a serious problem [1]. Suppose antibiotic medications are used at high doses. In that case, they can cause toxicity in the blood and, if taken at low doses, can lead to increased bacterial resistance at the site of infection [2]. In this case, antibiotics become ineffective at killing bacteria. Based on these problems, an alternative nanoparticle material with an antibacterial effect is needed to replace antibiotics [3]. In particular, metal oxide nanoparticles have great opportunities for antibacterial applications [4]. In this case, nano-

sized metal oxide materials that have received widespread attention in previous studies are iron oxide (Fe_3O_4) and zinc oxide (ZnO) nanoparticles [5].

Fe3O4 nanoparticles are superparamagnetic iron oxide with good separation properties from solution due to their magnetic potential. These magnetic properties are essential in biomedical applications that can inhibit and kill pathogenic bacteria [6]. However, these nanoparticles have high aggression and oxidation, which can cause deformation of the crystal structure [7]. Therefore, these Fe3O4 need to be surface modified for better stability. So alternative materials are required to improve the surface layer of Fe3O4 [8]. In this case, one of the biocompatible materials that can use in biomedical applications is zinc oxide (ZnO) nanoparticles [9-10]. ZnO nanoparticles are n-type semiconductor materials with a wide band gap of 3.1 – 3.3 eV and vibrant energy of 60 meV at room temperature [11]. ZnO nanoparticles' properties include good selectivity, low toxicity, heat resistance, and high stability [12]. ZnO nanoparticles have been previously investigated as non-toxic to human cells [13]. Thus, incorporating Fe3O4 nanoparticles as a filler and ZnO as a binder or matrix makes a nanocomposite material that can improve its structure and properties and act as an antibacterial agent that can form new compounds [14].

Nanoparticles Fe3O4 coated with ZnO (Fe3O4/ZnO) give better results in the biomedical field because of the biocompatible (non-toxic) nature of ZnO, which quickly penetrates cells, increases the durability of the catalyst, and can reduce the aggregation Fe3O4 nanoparticles [13]. Metal oxide nanocomposites exhibit good antibacterial properties and inhibit Escherichia coli bacteria's growth (gram-negative). and Staphylococcus aureus (gram-positive) [15]. Roeinfard & Bahari (2017) investigated the antimicrobial properties of Fe3O4/ZnO nanocomposite using the sol-gel method with a molar ratio of 1:10 and 1:20, proving that at a percentage of 1:10, it showed promising results used as a treatment application in cancer cells MCF-7. Madhubala & Kalaivani's (2018) report studied Fe3O4/ZnO nanocomposites with ratios of 1:5, 1:10, and 1:20. It has been known that inhibiting bacterial growth is best shown in a ratio of 1:10. Likewise to the research of Arunima Rajan et al. (2019), Fe3O4/ZnO/rGO nanocomposite by hydrothermal method shows the best antibacterial activity at a concentration of 1 mg/ml. Meanwhile, Thanh et al. (2020) study the ultrasonic-coprecipitation process. He demonstrated the effectiveness of antibacterial applications at a concentration of 1 mg/ml Fe3O4/ZnO/chitosan nanocomposite.

Various methods have been widely used to synthesize Fe3O4/ZnO nanocomposites. It including hydrothermal [1], ultrasonication [17], coprecipitation [18], and sol-gel [19], sonochemical [20], and biosynthetic [21]. The ultrasonication method has not been carried out of the several methods mentioned. The ultrasonication method is a method that utilizes high-frequency ultrasonic waves that are radiated into a solution so that it will cause collisions between particles to break large crystal aggregates into small crystal aggregates up to nanoscale. In addition, this method is effective, inexpensive, and environmentally friendly and requires a short time of experimentation [17]. Based on the results above, we researched to analyze Fe3O4/ZnO nanocomposites using ultrasonication. It has a weight ratio of Fe3O4: ZnO of 1:5, 1:10, and 1:15, which can be applied for antibacterial. The existence of different mass variations of ZnO aims to observe the best performance of nanocomposites from those studied previously. And can determine the formed phase, elemental analysis and

antimicrobial properties after the Fe3O4/ZnO composite is formed. The synthesis results will be analyzed using X-Ray Diffraction (XRD), Fourier transforms infrared (FTIR) and antibacterial test.

Experimental Method

The materials needed in the research are Tulungagung mineral sand, 37% HCl (Merck), 12 M NaOH, ZnO (smart-lab), water distilled, filter paper and aluminium foil. At the same time, the equipment used in this research is a magnet, digital balance, beaker glass, spatula, hotplate stirrer, funnel, Erlenmeyer flask, ultrasonic cleaner and oven.

Fe_3O_4 nanoparticles were synthesized using the coprecipitation method, referring to the research of Hefdea & Rohmawati (2020); Tulungagung mineral sand was separated using a bar magnet as much as 20 grams. Then it was dissolved with 53 ml of 37% HCl at 70^0C. The solution formed was filtered using filter paper, and the filtrate was titrated with 12M NaOH at 70^0C until a precipitate was formed. Furthermore, the precipitate formed was rinsed with distilled water then filtered and put in an oven at 100^0C for 3 hours.

The commercial product Zinc Oxide (ZnO) was prepared to prepare Fe_3O_4/ZnO nanocomposites with a ratio of 1:5, 1:10 and 1:15. The first step is 1 gram of Fe_3O_4 in ultrasonication for 30 minutes with a frequency of 40 kHz. Then the solution is stirred by adding ZnO until the solution is mixed. After that, let stand until the water content and sediment are separated. It removed the water content, and the precipitate was filtered in an oven at 90^0C for 3 hours.

The structural properties of Fe_3O_4, ZnO and Fe_3O_4/ZnO were observed using the PAN analytical X'pert PRO system X-ray diffraction. The characterization XRD has an operation of Cu-Kα 1.5406, voltage 40 kV, current 30 mA and 2θ angle range 10°- 80°. The phase composition and crystallinity of the synthesized results formed in the sample were identified using Qual-X and Origin software for later analysis. Calculations were carried out using the Debye-Scherrer to determine the average crystal size, such as:

$$D = \frac{0.89\,\lambda}{\beta \cos\theta} \qquad [1]$$

Where D is the crystal size in nm, λ is the X-ray wavelength in nm, β is the width of the highest peak at half the height in radians, and θ is the most increased peak diffraction angle in degrees. the calculation of the degree of crystallinity is calculated through the origin program and microsoft excel with the formula:

$$crystallinity\ (\%) = \frac{Total\ area\ of\ main\ peaks}{total\ area\ of\ all\ peaks}\ x\ 100\% \qquad [2]$$

Then the samples in powder form were tested for FTIR (Fourier Transform Infrared) type Shimadzu FTIR-8400 to determine the functional groups and absorption peaks with a wave number range of 400 - 4000 cm^{-1}. The output data from the FTIR is obtained as a graph of the relationship between transmittance and wavenumber. An Antibacterial activity test was carried out to determine the inhibition zone of bacterial activity in the sample using the Kirby Bauer disk diffusion method using two bacteria, Escherichia coli (Gram-negative) and Staphylococcus aureus (Gram-positive), with concentrations of 0.8 and 1 mg/ml. This sample was dissolved in water distilled and then ultrasonicated for 30 minutes by

sterilization through UV irradiation. The paper disc is wholly immersed in the solution. The suspension of the two bacteria (OD600 nm 0.1) was put in 100 µl in a petri dish and rubbed on the surface of Muller Hinton Agar (MHA) media with a cotton swab sterile. It placed a paper disk containing 20 µl of the test compound with a specific concentration on the surface of the MHA. Incubation was carried out for 24 hours at a temperature of 30°C. The clear zone formed around the disc was expressed as the inhibitory power of the compound against bacterial growth. This estimated results regarding the area of inhibition with a calliper in millimetres.

Result and Discussion

XRD Characterization

The data of the results of XRD to analyse determine the phase, crystal structure, and crystal size of Fe_3O_4, ZnO and Fe_3O_4/ZnO. Figure 1(a) diffraction peaks of Fe_3O_4 are located at 2θ = 30.11°, 35.58°, 43.10°, 56.91° and 62.58°. It is indicated by the hkl indices (220), (311), (400), (511) and (440), respectively. The maximum diffraction peak of Fe_3O_4 is located at an angle of 35.58° with crystal orientation (311). This diffraction angle corresponds to the JCPDS card number 00-900-5837, proving that Fe_3O_4 has an inverted cubic spinel structure, is in the space group Fd3m (227) and shows a magnetite phase. Crystal size results from Fe_3O_4 formula Debye-Scherrer of 42 nm and produces a degree of crystallinity of 47,08%.

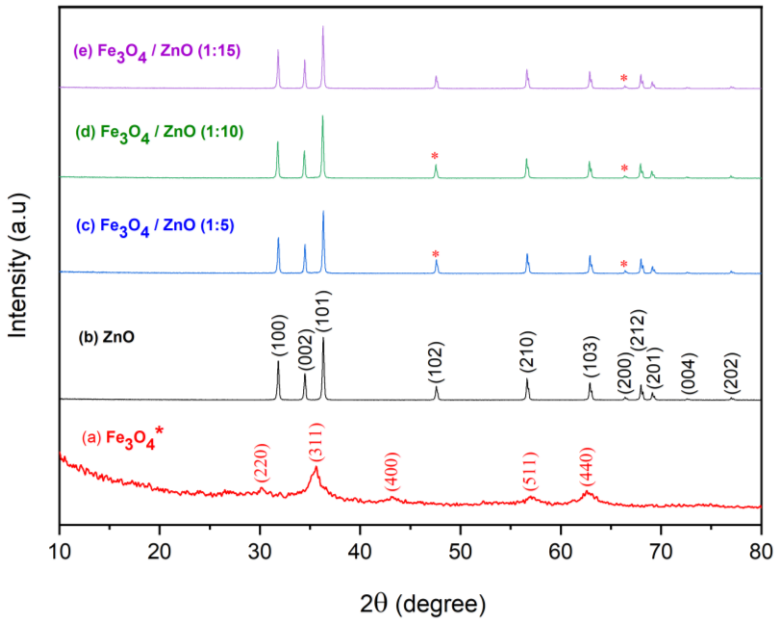

Figure 1. Sample XRD characterization results of (a) Fe_3O_4 (b) ZnO and nanocomposite Fe3O4/ZnO (c) 1:5 (d) 1:10 (e) 1:15

In Figure 1(b), the eleven diffraction peaks of ZnO nanoparticles are located at angles of 2θ = 31.82°, 34.48°, 36.31°, 47.59°, 56.64°, 62.90°, 66.42°, 67.99°, 69.12°, 72.60°, 76.99° with hkl values (100), (002), (101), (102), (110), (103), (112) and (201). The maximum diffraction peak is at 36.31° with the hkl plane (101), according to JCPDS card number 00-900-4178. The angle shows that ZnO has a hexagonal structure, is in the space group P63mc (186) and a zincite phase. The results obtained found the average crystal size to be 36.76 nm and produces a degree of crystallinity of 52,92%.

The diffraction peak of Fe_3O_4/ZnO nanocomposite was observed in Figure 1 (c-e). The rise that confirms the presence of Fe_3O_4 nanoparticles in Fe_3O_4/ZnO nanocomposites is indicated by an asterisk (*). The greater the mass of ZnO, the more Fe_3O_4 is on the nanocomposite surface, which can be seen in Figure 1. However, distinguishing the three nanocomposite samples lies in the magnitude of the intensity. It stands out at 36.31˚ for 1:5, 36.28˚ for 1:10, and 36.25˚ for 1:15 nanocomposites Fe_3O_4/ZnO. It can see in graph 1 that as the mass of ZnO increases, the presence of Fe_3O_4 disappears on the nanocomposite surface. The magnitude of the intensity stands out at an angle of 36.31˚ for 1:5, 36.28° for 1:10, and 36.25° for 1:15. It indicates of peak indicating the presence of Fe_3O_4 on the nanocomposite surface decreases with increasing ZnO concentration from a ratio of 1:5 to 1:15. This result also proves that in the largest nanocomposite (Fe_3O_4/ZnO 1:15), the crystal size decreased significantly as the mass ratio of ZnO increased. It implies that the Fe_3O_4 is wholly covered by the ZnO surface [16].

FTIR Characterization

The results of FTIR characterization on Fe_3O_4, ZnO, and Fe_3O_4/ZnO samples (1:15) are shown in Figure 2. The FTIR test was carried out using infrared spectroscopy to determine the functional groups in the bonds of organic and inorganic compounds in wavenumber values of 4000 - 400 cm^{-1}.

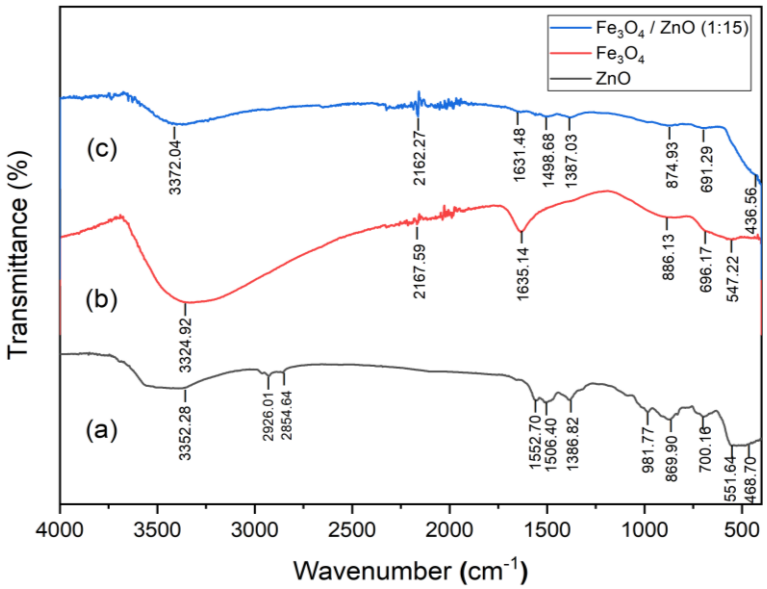

Figure 2. FTIR characterization of (a) ZnO (b) Fe_3O_4 (c) Fe_3O_4/ZnO (1:15)

In Figure 2(a), the absorption tape of the Zn−O bond is found at a wave number of 468.70 cm^{-1} [23]. While Figure 2(b) demonstrated the presence of iron structures in the synthesis of nanoparticles, a Fe−O compound bond is located at a wave number of 547.22 cm^{-1} [11]. In Figure 2(c), the absorbance peaks at wave numbers 3372.04 cm^{-1} and 1631.48 cm^{-1} show the organic compound bonds determined by the strain vibrations and bending vibrations of the OH hydroxyl group due to water absorbance vibrations [16,24,25].

Table 1. Functional group of Fe_3O_4/ZnO nanocomposites

No	Peak from synthesis (cm^{-1})	Peak from references (cm^{-1})	Bond type	References
1	3372.04	3400	O-H *stretching*	[2]
2	2162.27	2344 , 2360	C=O	[3][2]
3	1631.48	1630 ,1633	O-H *bending*	[4][2]
4	1498.68 , 1387.03	1479 , 1368	C=O	[5][3]
5	874.93	864 , 898	Fe-O *tetrahedral*	[6][7]
6.	691.29	676 , 716	Fe-O *octahedral*	[3][7]
7.	436.56	430 , 443, 450, 453	Zn-O	[4][2][5][8]

Antibacterial Activity Test

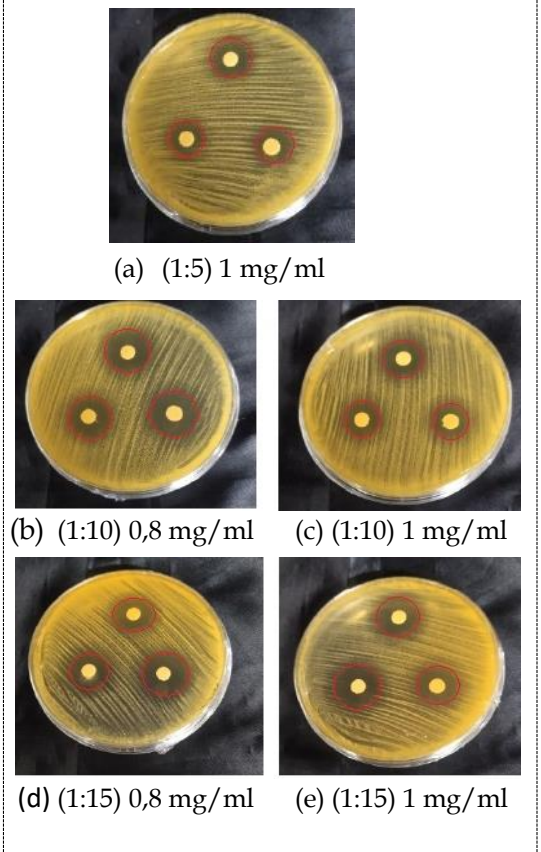

Figure 3. Inhibition zone of antibacterial activity formed on Fe_3O_4/ZnO nanocomposite on bacteria *S. aureus*

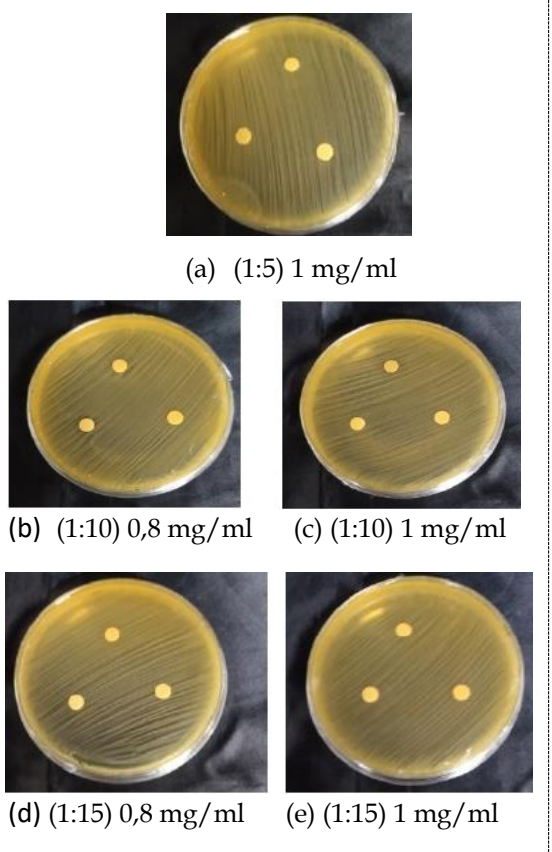

Figure 4. Inhibition zone of antibacterial activity formed on Fe_3O_4/ZnO nanocomposite on bacteria *E. coli*

Furthermore, the vibration peak appears at wave number 2162.27 cm^{-1}, which identifies the shape of the CO_2 in the air [26-27]. At wave numbers around 1498.68 cm^{-1} and 1387.03 cm^{-1}, a strain vibration of the C=O bond occurs during the synthesis process of reactive carbon [28]. New absorption peaks appeared on the nanocomposite surface at 874.93 cm^{-1} and 691.29 cm^{-}

^{1}, indicating the presence of oxygen and iron vibrations identified as characteristic peaks of Fe-O groups [1,20,23]. While at a wave number of about 436.56 cm^{-1} confirms the presence of Zn-O compound bonds on the nanocomposite surface [29]. For more details, in Table 1 below, the experimental results of the Fe_3O_4/ZnO nanocomposite functional group data are presented, and various references from previous research results are compared.

The antibacterial effectiveness of the three Fe_3O_4/ZnO samples could be observed by antibacterial testing using the disc diffusion method on *S. aureus* (Figure 3) and *E. coli* (Figure 4) bacteria with two different concentrations (0.8 and 1 mg/ml). The appearance of a clear zone characterized the disc diffusion method after 24 hours of incubation around the surface of the Fe_3O_4/ZnO. The antibacterial test results showed that the Fe_3O_4/ZnO had a higher inhibitory effect on the growth of *S. aureus* bacteria than *E. coli* bacteria. It can see that the antibacterial properties in the composite are indicated by the presence of ZnO [30]. As we know, ZnO is a metal oxide that provides antibacterial effects in various ways, for example, the formation of reactive oxygen species (ROS) and cell wall damage due to localized interactions of ZnO [13]. The diameter of the clear zone of antibacterial activity is shown in Table 2.

Tabel 2. Inhibition zone of nanocomposite samples on *E. coli* and *S. aureus* bacteria with concentrations of 0.8 and 1 mg/ml**.**

Nanocomposite	Concentration of nanocomposites (mg/ml)	Zone of inhibition (mm)	
		E. coli	***S.aureus***
Fe_3O_4/ZnO (1:5)	1	6.17 ± 0.28	12.98 ± 0.73
Fe_3O_4/ZnO (1:10)	0,8	6.63 ± 0.43	17.13 ± 0.24
	1	6.70 ± 0.23	14.28 ± 1.70
Fe_3O_4 /ZnO (1:15)	0,8	6.58 ± 0.23	16.62 ± 1.15
	1	6.65 ± 0.10	16.55 ± 1.35

Table 2 shows the most effective antibacterial test for *S. aureus* bacteria with an inhibition zone of (17.13 ± 0.24) mm at a 0.8 mg/ml concentration. Meanwhile, *E. coli* has a relatively small inhibition zone (6.70 ± 0.23) at 1 mg/ml concentration. Both bacteria showed the highest average inhibition zone in the Fe_3O_4/ZnO nanocomposite sample (1:10). These results indicate that Fe_3O_4/ZnO (1:10) nanocomposite is an excellent inhibitor against pathogenic bacteria. Previous studies at a 1:10 nanocomposite ratio showed promising results in toxicity tests [11,16,19]. In the table, it can observe that the bacterial inhibition zone increased in *E. coli* along with the increase in the ratio and concentration of nanocomposites.

Meanwhile, the nanocomposites, which showed antibacterial activity with the largest inhibition zone, were seen in *S. aureus* bacteria. The results of this study follow previous studies showing that *S. aureus* bacteria had higher resistance than *E. coli* [3,31,32]. This is because the high ZnO composition allows the presence of negatively charged free radicals, namely peroxide ions, and superoxide anions. It can be caused cell damage and death by *S. aureus* at a lower concentration (0.8 mg/ml) than *E. coli* which was only effective in killing bacteria found in Fe_3O_4 [33-34]. Thus, the high antibacterial effectiveness against *S. aureus* in Fe_3O_4/ZnO (1:10) nanocomposites is believed to cure infectious diseases caused by bacteria, for example, from skin infections, endocarditis and toxic shock syndrome (TSS) [32].

Conclusion

Fe_3O_4/ZnO nanocomposites were successfully synthesized using the ultrasonication method in this research. The results of the XRD analysis showed that the average size of Fe_3O_4 crystal was 42 nm, ZnO was 36 nm, and the average nanocomposite size was 39 nm. FTIR results on the surface of the nanocomposite showed that the characteristics of the Fe-O group could be identified at the absorption peak of 874.93 and 691.29 cm^{-1} while at a wave number of about 436.56 cm^{-1} indicated the presence of Zn-O compound bonds. The best bacterial growth inhibition effectiveness was found in *S. aureus* bacteria at 17.13 mm in Fe_3O_4/ZnO (1:10) nanocomposite at a 0.8 mg/ml concentration. This nanocomposite material can be applied to antibacterial applications.

Acknowledgment

The authors would like to thank the Materials Laboratory of the Department of Physics Universitas Negeri Surabaya, Laboratory of Minerals and Advanced Materials Universitas Negeri Malang, Laboratory of Materials and Metallurgy Institut Teknologi Sepuluh Nopember, Laboratory of Microbiology Universitas Airlangga which has provided facilities for research activities to sample testing.

References

[1] S. Arunima Rajan, A. Khan, S. Asrar, H. Raza, R. K. Das, and N. K. Sahu, "Synthesis of ZnO/Fe3O4/rGO nanocomposites and evaluation of antibacterial activities towards E. coli and S. aureus," *IET Nanobiotechnology*, vol. 13, no. 7, pp. 682–687, 2019, doi: 10.1049/iet-nbt.2018.5330.

[2] E. Guillot *et al.*, "Suboptimal Ciprofloxacin Dosing as a Potential Cause of Decreased Pseudomonas aeruginosa Susceptibility in Children with Cystic Fibrosis," *Pharmacother. J. Hum. Pharmacol. Drug Ther.*, vol. 30, no. 12, pp. 1252–1258, Dec. 2010, doi: 10.1592/PHCO.30.12.1252.

[3] T. Gordon, B. Perlstein, O. Houbara, I. Felner, E. Banin, and S. Margel, "Synthesis and characterization of zinc/iron oxide composite nanoparticles and their antibacterial properties," *Colloids Surfaces A Physicochem. Eng. Asp.*, vol. 374, no. 1–3, pp. 1–8, 2011, doi: 10.1016/j.colsurfa.2010.10.015.

[4] A. Azam, A. S. Ahmed, M. Oves, M. S. Khan, S. S. Habib, and A. Memic, "Antimicrobial activity of metal oxide nanoparticles against Gram-positive and Gram-negative bacteria: a comparative study," *Int. J. Nanomedicine*, vol. 7, pp. 6003–6009, 2012, doi: 10.2147/IJN.S35347.

[5] N. Beyth, Y. Houri-Haddad, A. Domb, W. Khan, and R. Hazan, "Alternative antimicrobial approach: Nano-antimicrobial materials," *Evidence-based Complement. Altern. Med.*, vol. 2015, 2015, doi: 10.1155/2015/246012.

[6] L. S. Arias, J. P. Pessan, A. P. M. Vieira, T. M. T. De Lima, A. C. B. Delbem, and D. R. Monteiro, "Iron Oxide Nanoparticles for Biomedical Applications: A Perspective on Synthesis, Drugs, Antimicrobial Activity, and Toxicity," *Antibiot. (Basel, Switzerland)*, vol. 7, no. 2, Jun. 2018, doi: 10.3390/ANTIBIOTICS7020046.

[7] M. Mahmoudi, S. Sant, B. Wang, S. Laurent, and T. Sen, "Superparamagnetic iron oxide nanoparticles (SPIONs): Development, surface modification and applications in chemotherapy," *Adv. Drug Deliv. Rev.*, vol. 63, no. 1–2, pp. 24–46, Jan. 2011, doi: 10.1016/J.ADDR.2010.05.006.

[8] W. S. Cho *et al.*, "Predictive value of in vitro assays depends on the mechanism of toxicity of metal oxide nanoparticles," *Part. Fibre Toxicol.*, vol. 10, no. 1, pp. 1–15, Oct. 2013, doi: 10.1186/1743-8977-10-55/TABLES/4.

[9] J. Gupta, P. A. Hassan, and K. C. Barick, "Core-shell Fe3O4@ZnO nanoparticles for magnetic hyperthermia and bio-imaging applications," *AIP Adv.*, vol. 11, no. 2, 2021, doi: 10.1063/9.0000135.

[10] T. Dayakar., K. Venkateswara Rao., K. Bikshalu., V. Rajendar., and S. H. Park, "Novel synthesis and structural analysis of zinc oxide nanoparticles for the non enzymatic glucose biosensor," *Mater. Sci. Eng. C. Mater. Biol. Appl.*, vol. 75, pp. 1472–1479, Jun. 2017, doi: 10.1016/J.MSEC.2017.02.032.

[11] M. Roeinfard and A. Bahari, "Nanostructural Characterization of the Fe3O4/ZnO Magnetic Nanocomposite as an Application in Medicine," *J. Supercond. Nov. Magn.*, vol. 30, no. 12, pp. 3541–3548, 2017, doi: 10.1007/s10948-017-4154-x.

[12] K. M. Lee, C. W. Lai, K. S. Ngai, and J. C. Juan, "Recent developments of zinc oxide based photocatalyst in water treatment technology: A review.," *Water Res.*, vol. 88, pp. 428–448, Oct. 2015, doi: 10.1016/J.WATRES.2015.09.045.

[13] A. Sirelkhatim *et al.*, "Review on Zinc Oxide Nanoparticles: Antibacterial Activity and Toxicity Mechanism," *Nano-micro Lett.*, vol. 7, no. 3, pp. 219–242, Apr. 2015, doi: 10.1007/S40820-015-0040-X.

[14] J. Zhou, N. Xu, and Z. L. Wang, "Dissolving behavior and stability of ZnO wires in biofluids: A study on biodegradability and biocompatibility of ZnO nanostructures," *Adv. Mater.*, vol. 18, no. 18, pp. 2432–2435, 2006, doi: 10.1002/adma.200600200.

[15] M. S. Barreto, C. T. Andrade, E. G. Azero, V. M. Paschoalin, and E. M. Del Aguila, "Production of Chitosan/Zinc Oxide Complex by Ultrasonic Treatment with Antibacterial Activity," *J. Bacteriol. Parasitol.*, vol. 08, no. 05, 2017, doi: 10.4172/2155-9597.1000330.

[16] V. Madhubala and T. Kalaivani, "Phyto and hydrothermal synthesis of Fe 3 O 4 @ZnO core-shell nanoparticles using Azadirachta indica and its cytotoxicity studies," *Appl. Surf. Sci.*, vol. 449, pp. 584–590, 2018, doi: 10.1016/j.apsusc.2017.12.105.

[17] V. M. Thanh, N. T. Huong, D. T. Nam, N. D. T. Dung, Le Van Thu, and M. T. Nguyen-Le, "Synthesis of ternary Fe3O4/ZnO/chitosan magnetic nanoparticles via an ultrasound-assisted coprecipitation process for antibacterial applications," *J. Nanomater.*, vol. 2020, 2020, doi: 10.1155/2020/8875471.

[18] M. Shashank, H. S. B. Naik, G. Nagaraju, R. S. Keri, M. M. Naik, and K. Lingaraju, "Facile Synthesis of Fe3O4/ZnO Nanocomposite: Applications to Photocatalytic and Antibacterial Activities," *J. Electron. Mater.*, vol. 50, no. 6, pp. 3557–3568, 2021, doi:

10.1007/s11664-021-08816-9.

[19] A. Bahari, M. Roeinfard, A. Ramzannezhad, M. Khodabakhshi, and M. Mohseni, "Nanostructured Features and Antimicrobial Properties of Fe 3 O 4 /ZnO Nanocomposites," *Natl. Acad. Sci. Lett.*, vol. 42, no. 1, pp. 9–12, 2019, doi: 10.1007/s40009-018-0666-6.

[20] H. Nurul Ulya, A. Taufiq, and Sunaryono, "Comparative Structural Properties of Nanosized ZnO/Fe3O4 Composites Prepared by Sonochemical and Sol-Gel Methods," *IOP Conf. Ser. Earth Environ. Sci.*, vol. 276, no. 1, pp. 2–11, 2019, doi: 10.1088/1755-1315/276/1/012059.

[21] M. Ghasemian Dazmiri, H. Alinezhad, Z. Hossaini, and A. R. Bekhradnia, "Green synthesis of Fe3O4/ZnO magnetic core-shell nanoparticles by Petasites hybridus rhizome water extract and their application for the synthesis of pyran derivatives: Investigation of antioxidant and antimicrobial activity," *Appl. Organomet. Chem.*, vol. 34, no. 9, p. e5731, Sep. 2020, doi: 10.1002/AOC.5731.

[22] P. S. Fisika and U. N. Surabaya, "Sintesis Fe 3 O 4 dari Pasir Mineral Tulungagung Menggunakan Metode Kopresipitasi," vol. 09, pp. 2015–2018, 2020.

[23] O. D. Maynez-Navarro, M. A. Mendez-Rojas, D. X. Flores-Cervantes, and J. L. Sanchez-Salas, "Hydroxyl Radical Generation by Recyclable Photocatalytic Fe3O4/ZnO Nanoparticles for Water Disinfection," *Air, Soil Water Res.*, vol. 13, 2020, doi: 10.1177/1178622120970954.

[24] A. Ahadpour Shal and A. Jafari, "Study of Structural and Magnetic Properties of Superparamagnetic Fe3O4–ZnO Core–Shell Nanoparticles," *J. Supercond. Nov. Magn. 2014 276*, vol. 27, no. 6, pp. 1531–1538, Jan. 2014, doi: 10.1007/S10948-013-2469-9.

[25] J. Saffari, N. Mir, D. Ghanbari, K. Khandan-Barani, A. Hassanabadi, and M. R. Hosseini-Tabatabaei, "Sonochemical synthesis of Fe3O4/ZnO magnetic nanocomposites and their application in photo-catalytic degradation of various organic dyes," *J. Mater. Sci. Mater. Electron.*, vol. 12, no. 26, pp. 9591–9599, Dec. 2015, doi: 10.1007/S10854-015-3622-Y.

[26] M. Aliahmad and N. Nasiri Moghaddam, "Synthesis of maghemite (γ-Fe2O3) nanoparticles by thermal-decomposition of magnetite (Fe3O4) nanoparticles," *Mater. Sci. Pol.*, vol. 31, no. 2, pp. 264–268, Apr. 2013, doi: 10.2478/S13536-012-0100-6.

[27] H. M. Joseph and N. Poornima, "Synthesis and characterization of ZnO nanoparticles," *Mater. Today Proc.*, vol. 9, pp. 7–12, 2019, doi: 10.1016/j.matpr.2019.02.029.

[28] G. Xiong, U. Pal, J. G. Serrano, K. B. Ucer, and R. T. Williams, "Photoluminescence and FTIR study of ZnO nanoparticles: The impurity and defect perspective," *Phys. Status Solidi Curr. Top. Solid State Phys.*, vol. 3, no. 10, pp. 3577–3581, 2006, doi: 10.1002/pssc.200672164.

[29] Y. Wang *et al.*, "Facile fabrication of ZnO nanorods modified Fe3O4 nanoparticles with enhanced magnetic, photoelectrochemical and photocatalytic properties," *Opt. Mater. (Amst).*, vol. 111, no. September, p. 110608, 2021, doi: 10.1016/j.optmat.2020.110608.

[30] A. Jain, R. Bhargava, and P. Poddar, "Probing interaction of Gram-positive and Gram-negative bacterial cells with ZnO nanorods," *Mater. Sci. Eng. C*, vol. 33, no. 3, pp. 1247–1253, Apr. 2013, doi: 10.1016/J.MSEC.2012.12.019.

[31] P. Goyal, S. Chakraborty, and S. K. Misra, "Multifunctional Fe3O4-ZnO nanocomposites for environmental remediation applications," *Environ. Nanotechnology, Monit. Manag.*, vol. 10, pp. 28–35, 2018, doi: 10.1016/j.enmm.2018.03.003.

[32] S. Singh, K. C. Barick, and D. Bahadur, "Inactivation of bacterial pathogens under magnetic hyperthermia using Fe3O4-ZnO nanocomposite," *Powder Technol.*, vol. 269, pp. 513–519, 2015, doi: 10.1016/j.powtec.2014.09.032.

[33] N. Padmavathy and R. Vijayaraghavan, "Enhanced bioactivity of ZnO nanoparticles - An antimicrobial study," *Sci. Technol. Adv. Mater.*, vol. 9, no. 3, Jul. 2008, doi: 10.1088/1468-6996/9/3/035004.

[34] K. M. Reddy, K. Feris, J. Bell, D. G. Wingett, C. Hanley, and A. Punnoose, "Selective toxicity of zinc oxide nanoparticles to prokaryotic and eukaryotic systems," *Appl. Phys. Lett.*, vol. 90, no. 21, 2007, doi: 10.1063/1.2742324.